Materials Transactions, Vol. 46, No. 6 (2005) pp. 1407 to 1412

EXPRESS REGULAR ARTICLE

Effect of Mn or Co on Kinetics of Eutectoid Decomposition in Sintered α-Fe_2Si_5 Alloys

Junxiang Jiang, Kazuhiro Matsugi, Gen Sasaki and Osamu Yanagisawa

Graduate School of Engineering, Hiroshima University, Higashi-Hiroshima 739-8527, Japan

The evolution of the eutectoid decomposition, α-$Fe_2Si_5 \rightarrow \beta$-$FeSi_2 + Si$, in sintered α-Fe_2Si_5 alloys with added Mn or Co has been traced by measuring the electrical resistivity under isothermal conditions. The time-temperature-transformation (TTT) diagram was obtained for each alloy, and presents a typical C shape in the temperature range of 873–1148 K. The addition of Mn or Co decreases the overall transformation rate, prolonging both the induction and transformation periods. The kinetics of the eutectoid reaction is discussed in the theoretical framework of Johnson–Mehl–Avrami (JMA) theory. It was found that the transformation mechanism of the eutectoid reaction is not affected by the addition of Mn or Co, and the effective activation energy of the Mn- or Co-added alloy is the same as that of the non-doped alloy. The added Mn or Co causes the decrease in the pre-exponential constant K_0, which decreases the overall transformation rate.

(Received February 15, 2005; Accepted April 25, 2005; Published June 15, 2005)

Keywords: *thermoelectric material, resistivity measurements, kinetics of eutectoid decomposition, Johnson–Mehl–Avrami equation*

1. Introduction

Manganese (Mn)[1,2] and cobalt (Co)[2–4] are the most effective doping elements for p- and n-type β-$FeSi_2$ respectively, which are attractive thermoelectric materials for use in air at high temperatures.[1–4] The α-Fe_2Si_5 phase, proposed as a new composition instead of the stoichiometric $FeSi_2$,[5,6] undergoes a phase transition, $\alpha \rightarrow \beta + Si$, from a high-temperature metallic structure to a low-temperature semiconducting β-$FeSi_2$ phase at 1210 K according to the equilibrium phase diagram of the Fe–Si system[7] shown in Fig. 1. Several studies of the eutectoid reaction have been reported,[5,6,8–10] but a different mechanism was found for the solidified and sintered materials. Two-dimensional growth was proposed for the solidified alloys,[6,8] whereas, for the sintered materials, three-dimensional growth was found to control the eutectoid reaction in the non-doped α-Fe_2Si_5 alloy.[10] Although doping with Mn or Co was found to decrease the transformation rate,[5,6] its effect on the kinetics of the eutectoid reaction is still not well understood, especially for the sintered materials.

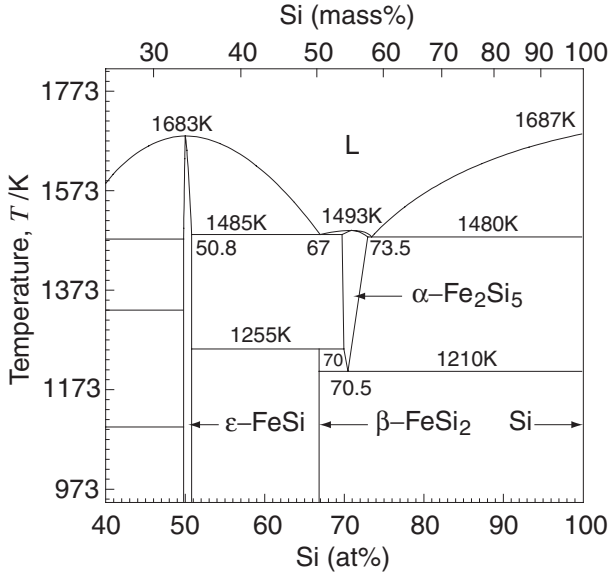

Fig. 1 Part of the equilibrium phase diagram of the Fe–Si system.

The Johnson–Mehl–Avrami (JMA) theory[11] is usually used to investigate the kinetics of the transformation in the solid state with isothermal experiments. Considering the spatial distribution (random, clustered or ordered) of the new phase, a general expression of the JMA equation was proposed by us,[10] in which the transformed volume fraction (X) of the product phase as a function of time (t) is given by

$$X^m(t) = 1 - \exp(-K^m t^{nm}), \tag{1}$$

where m is a constant covering all cases of the spatial distribution, in which a value of $m = 1$ represents random distribution, $m > 1$ ordered distribution and $m < 1$ clustered distribution, n is the Avrami exponent reflecting the characteristics of the nucleation and growth processes, and K is a thermally activated rate constant representing both nucleation and growth rates and assumed to have an Arrhenius temperature dependence,

$$K = K_0 \exp(-E_a/RT), \tag{2}$$

where K_0 is a pre-exponential term representing the frequency factor, E_a is the apparent activation energy with contributions from the activation energy of nucleation (E_N) and that of growth (E_G), R is the gas constant and T is the isothermal temperature in Kelvin.

The purpose of this study is to investigate the kinetics of eutectoid decomposition in sintered α-Fe_2Si_5 alloys with added Mn or Co with electrical resistivity measurements during isothermal annealing. The effect of Mn or Co addition on the kinetics of this reaction is discussed in the framework of JMA theory.

2. Experimental Procedure

Two alloys with the α-Fe_2Si_5 compositions listed in Table 1 were prepared from 99.9% purity electrolytic iron, manganese or cobalt and high purity silicon for semiconductors by levitation melting in a high-frequency in-

Table 1 JMA parameters for isothermal transformation in $Fe_{27.14}Mn_{2.36}Si_{70.5}$ and $Fe_{28.91}Co_{0.59}Si_{70.5}$ at different temperatures.

Composition	T/K	$\tau_{0.001}$/s	m	n	K/s^{-1}
$Fe_{27.14}Mn_{2.36}Si_{70.5}$	873	145068	0.94	3.09	1.02×10^{-16}
	923	53343	0.89	3.04	3.31×10^{-15}
	973	24008	0.88	3.06	3.46×10^{-14}
	1023	9138	0.90	3.09	4.17×10^{-13}
	1073	5038	0.90	2.98	9.36×10^{-13}
	1123	24840	0.90	3.65	3.38×10^{-17}
	1148	186145	0.89	3.77	5.02×10^{-19}
$Fe_{28.91}Co_{0.59}Si_{70.5}$	873	71159	0.87	3.01	4.03×10^{-15}
	923	24465	0.83	2.96	6.07×10^{-14}
	973	8612	0.90	2.98	1.17×10^{-12}
	1023	4314	0.88	2.94	1.30×10^{-11}
	1073	5492	0.85	3.33	1.13×10^{-13}
	1123	13359	0.89	3.71	3.79×10^{-17}
	1148	106619	0.84	3.87	1.03×10^{-21}

duction furnace under an argon gas atmosphere. The ingot was pulverized to −45 mesh and further mechanically ground with a planetary ball mill for 5 h. The powders were sintered in a graphite die at 1223 K for 30 min at 30 MPa by the spark plasma sintering method in vacuum. Specimens with dimensions of $2 \times 4 \times 18$ mm were cut and used in the experimental studies.

Resistivity experiments were carried out using a time-temperature cycle: heating up to the α homogenization field (1233 K); isothermally holding at this temperature for 10 min; rapidly cooling to the chosen holding temperature and then isothermally holding at this temperature. During the isothermal exposure, the electrical resistivity (ρ) was simultaneously measured by the standard four-probe d.c. method to trace the course of eutectoid transformation. The measurements were performed at different constant temperatures (T) from 873 to 1148 K under an argon atmosphere.

Some specimens were quenched in water from the intermediate stages of the isothermal annealing. The changes in microstructure were investigated by optical microscopy, electron probe micro-analysis (EPMA) and x-ray diffraction (XRD) analysis.

3. Results and Discussion

3.1 Microstructure

Figure 2 is an optical micrograph of the $Fe_{27.14}Mn_{2.36}Si_{70.5}$ alloy, presented to illustrate the evolution of the microstructure under isothermal annealing. The corresponding XRD analysis is shown in Fig. 3. As can be seen in Fig. 2(a), except for the pores left by the sintering process the as-sintered specimen presents a mono-phase structure, shown by XRD to be the α-Fe_2Si_5 phase [Fig. 3(a)]. Figure 2(b) shows the typical microstructure of the initial stage of the transformation in a specimen quenched in water after 3 h of annealing at 1073 K. The dark grey transformed regions are composed of β-$FeSi_2$ and Si phases, as confirmed by the peaks of these phases in Fig. 3(b) and by EPMA analysis. It can be seen that the transformed eutectoid grains are growing isotropically and are weakly clustered even in the early stages

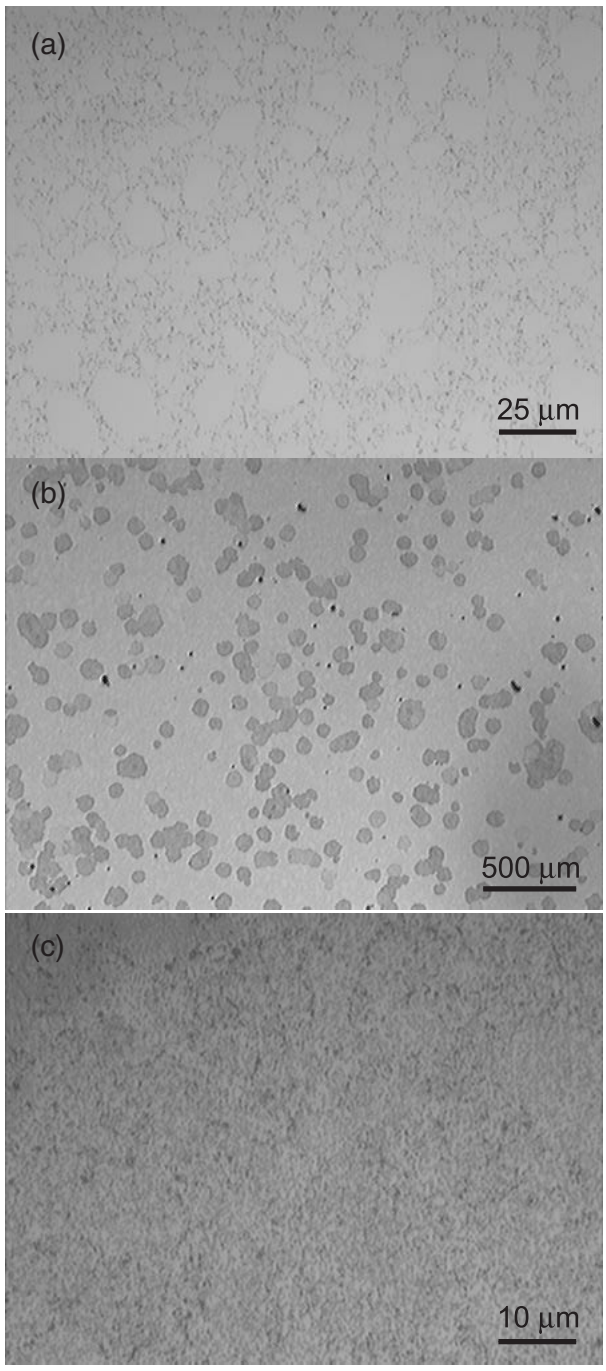

Fig. 2 Microstructural evolution of $Fe_{27.14}Mn_{2.36}Si_{70.5}$ under isothermal annealing. (a) As-sintered, (b) Annealed at 1073 K for 3 h, (c) Annealed at 1073 K for 20 h.

of the transformation. Figure 2(c) shows the microstructure of a specimen annealed at 1073 K for 20 h, and Fig. 3(c) shows the corresponding XRD pattern. As can be seen, there is no α phase remaining and the mono-phase structure has completely transformed to a duplex structure of β phase matrix and Si particles.

The evolution of the microstructure of the $Fe_{28.91}Co_{0.59}Si_{70.5}$ alloy in isothermal annealing presents the same characteristics as the $Fe_{27.14}Mn_{2.36}Si_{70.5}$ alloy.

3.2 Time dependence of electrical resistivity

Figures 4(a) and (b) show the electrical resistivity (ρ)

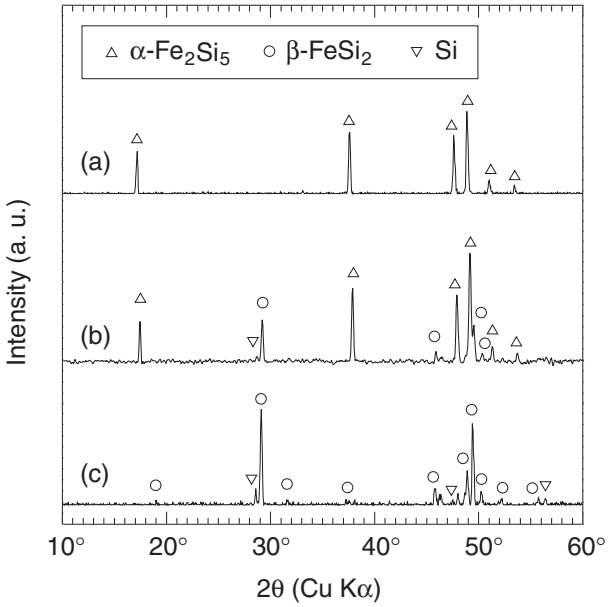

Fig. 3 X-ray diffraction patterns of $Fe_{27.14}Mn_{2.36}Si_{70.5}$. (a) As-sintered, (b) Annealed at 1073 K for 3 h, (c) Annealed at 1073 K for 20 h.

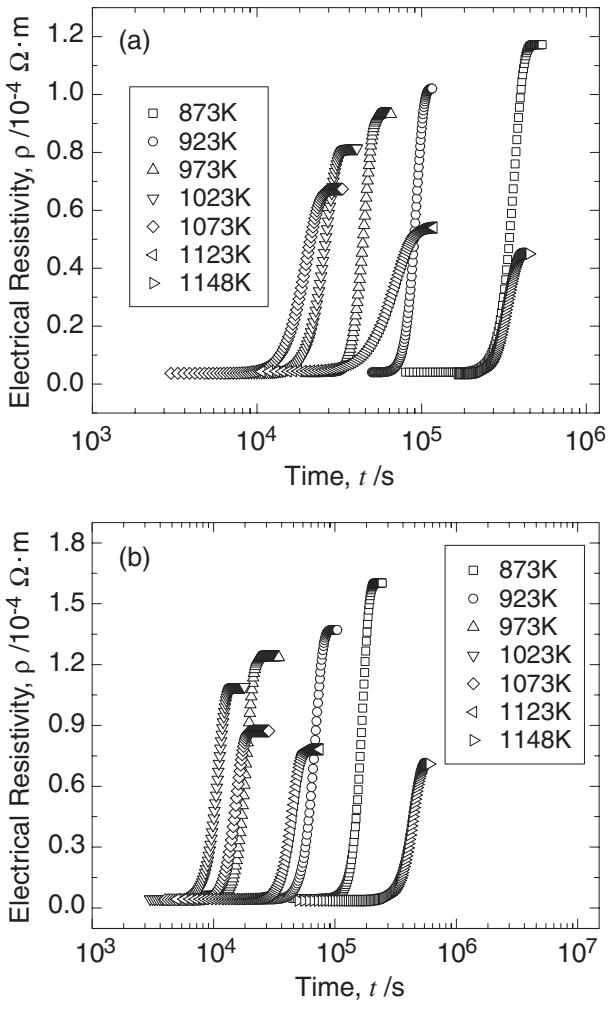

Fig. 4 Time dependence of the electrical resistivity under isothermal annealing at various temperatures. (a) $Fe_{27.14}Mn_{2.36}Si_{70.5}$ and (b) $Fe_{28.91}Co_{0.59}Si_{70.5}$.

versus annealing time (t) at various isothermal temperatures for $Fe_{27.14}Mn_{2.36}Si_{70.5}$ and $Fe_{28.91}Co_{0.59}Si_{70.5}$. The electrical resistivity curve presents the same characteristic sigmoidal shape at each temperature. During isothermal treatment, the electrical resistivity remains almost constant in the first stage of annealing, then increases sharply with time and finally reaches its equilibrium value. For both alloys, the equilibrium value of ρ at the final stage decreases with increasing annealing temperature, which indicates semiconducting characteristics because the transformed phases are semiconductors.

3.3 Time-Temperature-Transformation (TTT) diagram

The measured resistivity signal $\rho(t)$ was transformed to a volume fraction $X(t)$ for each temperature using the relationship between ρ and X proposed for a two-phase composite,[12]

$$\frac{1}{\rho_c} = \frac{f_\alpha^r}{\rho_\alpha} + \frac{f_\beta^s}{\rho_\beta} + \frac{(1 - f_\alpha^r - f_\beta^s)^2}{\rho_\alpha(f_\alpha - f_\alpha^r) + \rho_\beta(f_\beta - f_\beta^s)}$$

where ρ_c, ρ_α and ρ_β are the electrical resistivity of composite, α phase and β phase respectively, f_α and f_β are the volume fraction of α and β respectively, and r and s are the constants characterizing the phase arrangement in microstructure and determined to be 1.268 and 3.536 respectively in our previous work.[10]

The transformed volume fraction was plotted in the time-temperature-transformation (TTT) diagram, which gives the relationship between the temperature (plotted linearly) and the time (plotted logarithmically) for fixed fractional amounts of transformation to be attained. Such TTT diagrams for the sintered $Fe_{27.14}Mn_{2.36}Si_{70.5}$ and $Fe_{28.91}Co_{0.59}Si_{70.5}$ alloys within the temperature range of 873–1148 K are shown in Figs. 5(a) and (b). However, it should be noted that the times corresponding to the beginning and end of transformation cannot really be measured experimentally. For this reason we show the transformed fractions of 2 and 98% for the beginning and end of the transformation respectively. The shape of the curves can typically be described by the character C for both alloys. The nose temperature obtained is about 1073 K for the $Fe_{27.14}Mn_{2.36}Si_{70.5}$ alloy, which is the same as the non-doped alloy,[10] but which is decreased slightly to about 1048 K by the addition of 0.59 at% Co. A delayed onset of the reaction can be observed with the addition of Mn or Co and the transformation period, $X = 0.02$–0.98, is prolonged in the whole temperature range measured, especially with 2.36 at% added Mn. The same effect of Mn or Co addition on the transformation time was observed in the solidified materials.[6]

3.4 Kinetics of eutectoid decomposition

The kinetics of the reaction was analyzed within the framework of the Johnson–Mehl–Avrami (JMA) theory by using a modified form of eq. (1),

$$\frac{1}{m}\ln[-\ln(1 - X^m)] = \ln K + n \ln t. \quad (3)$$

This equation can be used to analyze the experimental data by means of logarithmic plots, where $\ln[-\ln(1 - X^m)]/m$ is plotted vs. $\ln t$. The slope of the resulting straight line is the

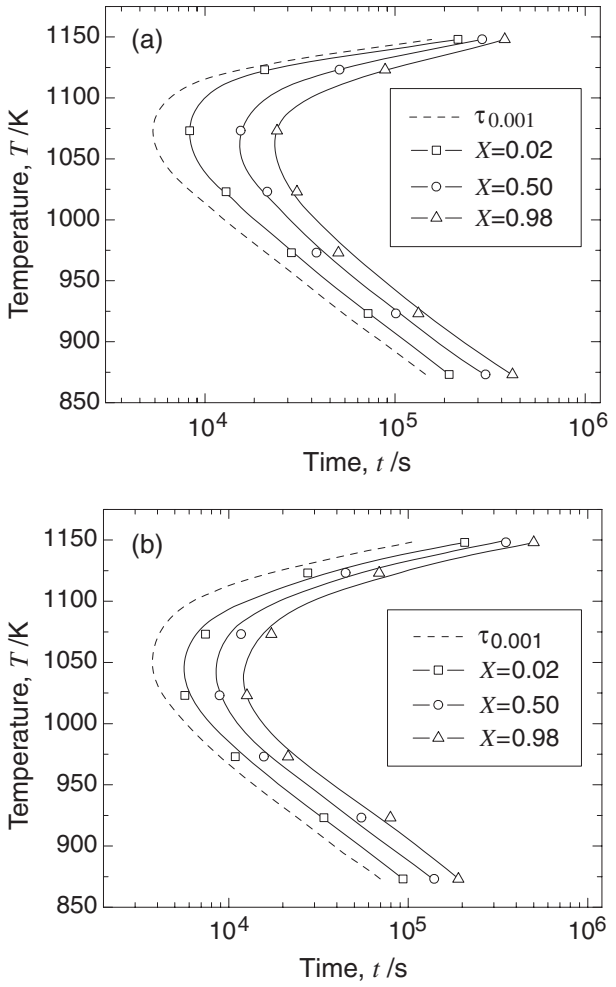

Fig. 5 Isothermal transformation diagram for $Fe_{27.14}Mn_{2.36}Si_{70.5}$ (a) and $Fe_{28.91}Co_{0.59}Si_{70.5}$ (b).

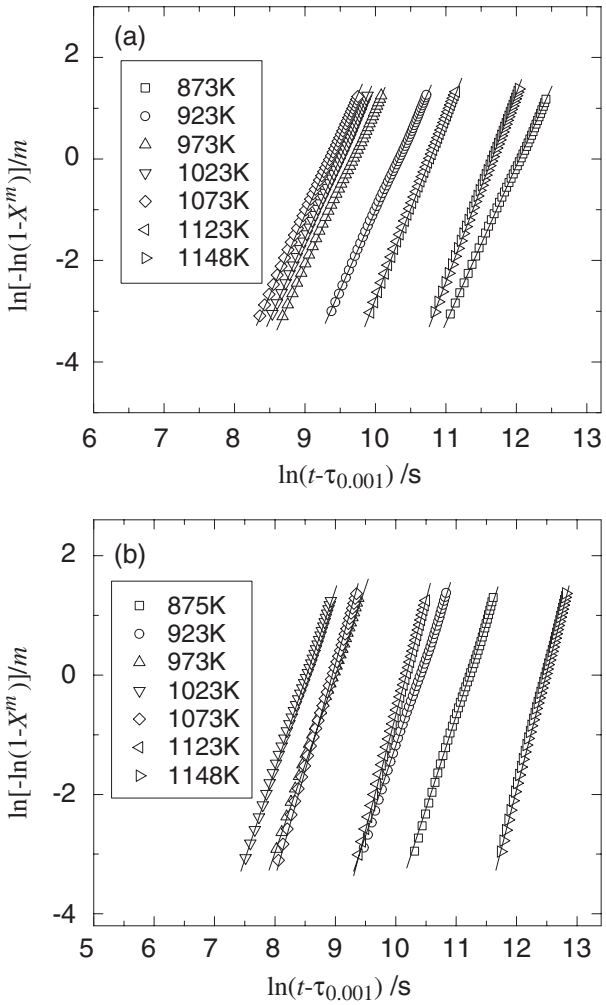

Fig. 6 Plots of $\ln[-\ln(1-X^m)]/m$ vs. $\ln(t-\tau_{0.001})$ for isothermal annealing at different temperatures. (a) $Fe_{27.14}Mn_{2.36}Si_{70.5}$ and (b) $Fe_{28.91}Co_{0.59}Si_{70.5}$.

Avrami exponent n, while the K value can be calculated from the intercept.

It should be emphasized that until now the direct estimation of m from the spatial distribution of product phases has not been sufficiently investigated. Fortunately, a value of $m < 1$ can be expected because a weak clustering of the transformed regions is observed in all samples annealed at different temperatures.

A linear fitting according to eq. (3) on the basis of least-squares regression was used to analyze the experimental data by taking into account the restriction that $m < 1$. Prior to the numerical data fitting, an induction period (τ) was introduced to correct the onset time of the transformation. Here, the formation time $\tau_{0.001}$, required to attain $X = 0.001$ and indicated by dashed lines in Fig. 5, is considered to be the induction time, and the value is listed in Table 1. To eliminate the measuring error in the beginning and final stages of the transformation, linear fitting was carried out in the region $X = 0.02$–0.98. The results of such fittings for the two alloys are shown in Fig. 6 by the plots of $\ln[-\ln(1-X^m)]/m$ vs. $\ln(t-\tau_{0.001})$. As can be seen, the experimental measurements are described very well by straight lines for all temperatures used. This means that eq. (1) can be applied to describe the kinetics of the eutectoid transformation in these alloys under isothermal conditions. The values of m, n, and K, derived from the linear fittings for all applied temperatures are also listed in Table 1.

The constant m takes an average value of about 0.9 for the $Fe_{27.14}Mn_{2.36}Si_{70.5}$ alloy and 0.86 for the $Fe_{28.91}Co_{0.59}Si_{70.5}$ alloy. Both values suggest weak clustering for the spatial distribution of the product phases. Since the eutectoid decomposition of the α phase begins almost entirely at surface irregularities such as cracks and flaws,[13] a weak clustering of nucleation will occur even in the sintered materials, in which many pores will remain during the sintering of the powders.

Taking experimental errors into account, the Avrami exponents in the low temperature region, below the nose temperature in the TTT diagram, can be assumed to be constant and equal to 3.0 for both alloys. However, above this temperature they will have values > 3.0. The value of $n \geq 3$ for all samples implies a three-dimensional growth of the new phase, which is in accordance with the results of microstructure observation. Below the nose temperature, the value of $n = 3.0$ implies that the growth rate alone controls the overall reaction rate after the nucleation sites become saturated in the early stages of the transformation.[11]

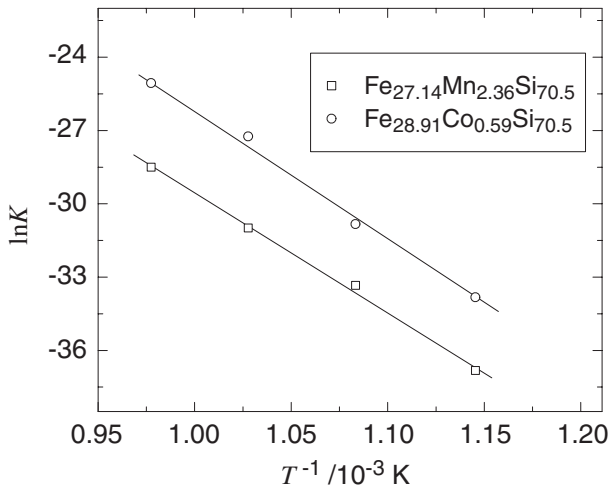

Fig. 7 Arrhenius plot of $\ln K$ vs. $1/T$ for isothermal annealing of $Fe_{27.14}Mn_{2.36}Si_{70.5}$ and $Fe_{28.91}Co_{0.59}Si_{70.5}$.

However, the value of $n > 3.0$ above the nose temperature indicates that three-dimensional growth occurs with a decreasing nucleation rate for the eutectoid reaction.[11] It can be seen that the transformation mechanism for the Mn- or Co-added alloy is the same as that of the non-doped sintered alloy whether above or below the nose temperature.[10]

On the other hand, the rate constant (K) is a function of temperature, as expected, increases with increasing annealing temperature within the low-temperature region below the nose temperature. The relationship between K and T is assumed to follow an Arrhenius dependence, as in eq. (2). Figure 7 shows Arrhenius plots of the rate constant $\ln K$ vs. $1/T$, linearly fitted by least-squares regression. The apparent activation energy (E_a) can be derived from the slope of the straight line, and the pre-exponential constant (K_0) from the intercept. Since n takes an integer value of 3.0 in this temperature region, the transformation will be controlled by the growth process alone and the apparent activation energy (E_a) is contributed only by the activation energy of growth (E_G) with $E_a = nE_G$.[14] Thus, the effective activation energy (E_c) for the eutectoid decomposition is equal to E_G ($= E_a/n$). The values of E_c and K_0 obtained in the transformation period, as compared with those of the non-doped alloy,[10] are listed in Table 2.

In the induction period of the reaction, the kinetics was examined by plotting $\ln t$ vs. $1/T$,[15,16] where $\ln t$ can be expressed by the following equation, obtained by inserting eq. (2) into eq. (3),

$$\ln t = \frac{1}{mn}\ln[-\ln(1-X^m)] - \frac{1}{n}\ln K_0 + \frac{E_a}{nRT}. \qquad (4)$$

Since the induction time $\tau_{0.001}$ covers the early stages of the transformation process, including the period of nucleus formation and the beginning of grain growth, the values of $\tau_{0.001}$ listed in Table 1 were used as t in eq. (4). In the corresponding plot of $\ln \tau_{0.001}$ vs. $1/T$ a linear fitting was carried out within the low-temperature region below the nose temperature. With the assumption that m and n values were the same as during the transformation period, the kinetic parameters, E_c and K_0, obtained in the induction period are also listed in Table 2, as well as those of the non-doped alloy.[10]

Table 2 Kinetic parameters for isothermal transformation of α-Fe_2Si_5 alloys. The induction period is $X = 0$–0.001; the transformation period is $X = 0.02$–0.98.

Composition	Induction Period		Transformation Period	
	K_0/s^{-1}	$E_c/kJ\cdot mol^{-1}$	K_0/s^{-1}	$E_c/kJ\cdot mol^{-1}$
$Fe_{29.5}Si_{70.5}$[10]	5.26×10^8	129.5	6.78×10^8	132.8
$Fe_{27.14}Mn_{2.36}Si_{70.5}$	1.85×10^6	134.8	2.45×10^8	135.4
$Fe_{28.91}Co_{0.59}Si_{70.5}$	1.75×10^8	135.0	5.19×10^8	133.0

The effective activation energy of the reaction changes notably neither with the addition of Mn or Co nor with the reaction period, and can be considered constant, although both the induction and transformation periods are prolonged by the addition of Mn or Co. It is clear that the effective activation energy is not the key reason for the decrease in the overall transformation rate. As discussed above, during the transformation period the reaction is controlled by the growth process alone, therefore, the increase in it can be attributed to the decrease in K_0 caused by the addition of Mn or Co, which decreases the growth rate according to eq. (2). However, the delay in the onset of the reaction is not only related to the growth rate but also related to the period of nucleus formation. It can be seen that during the induction period the K_0 for Co-added alloy shows a value as small as 1/3 of that of the non-doped alloy and K_0 for the Mn-added alloy is two orders of magnitude smaller. This marked decrease in K_0 could be the reason for the long time required to attain site saturation of nucleation in the early stages, by decreasing the nucleation rate. Thus the addition of Mn or Co not only decreases the growth rate during the transformation period but also decreases the nucleation rate during the induction period.

From the microstructure of the fully transformed samples annealed at 973 K shown in Fig. 8, it is seen that the grains in the $Fe_{27.14}Mn_{2.36}Si_{70.5}$ and $Fe_{28.91}Co_{0.59}Si_{70.5}$ alloys are notably larger than those in the non-doped $Fe_{29.5}Si_{70.5}$ alloy. A small quantity of nuclei may be one of the reasons for the decrease in K_0 in the alloy added with Mn or Co.

4. Conclusions

The eutectoid decomposition, $\alpha \rightarrow \beta + Si$, in sintered α-Fe_2Si_5 based alloys with added Mn or Co, was studied with resistivity measurements under isothermal conditions. The time-temperature-transformation (TTT) diagram for each alloy was obtained in the temperature range of 873–1148 K. The TTT diagrams show a typical C shape with a nose at 1073 K for the $Fe_{27.14}Mn_{2.36}Si_{70.5}$ alloy and 1048 K for the $Fe_{28.91}Co_{0.59}Si_{70.5}$ alloy. The addition of Mn or Co decreases the overall transformation rate, prolonging both the induction and transformation periods. The kinetic analysis suggests that Mn- and Co-added alloys have the same transformation mechanism and the same effective activation energy as the non-doped alloy. The decrease in the transformation rate is attributed to the decrease in the pre-exponential constant K_0, which causes a growth rate decrease during the transforma-

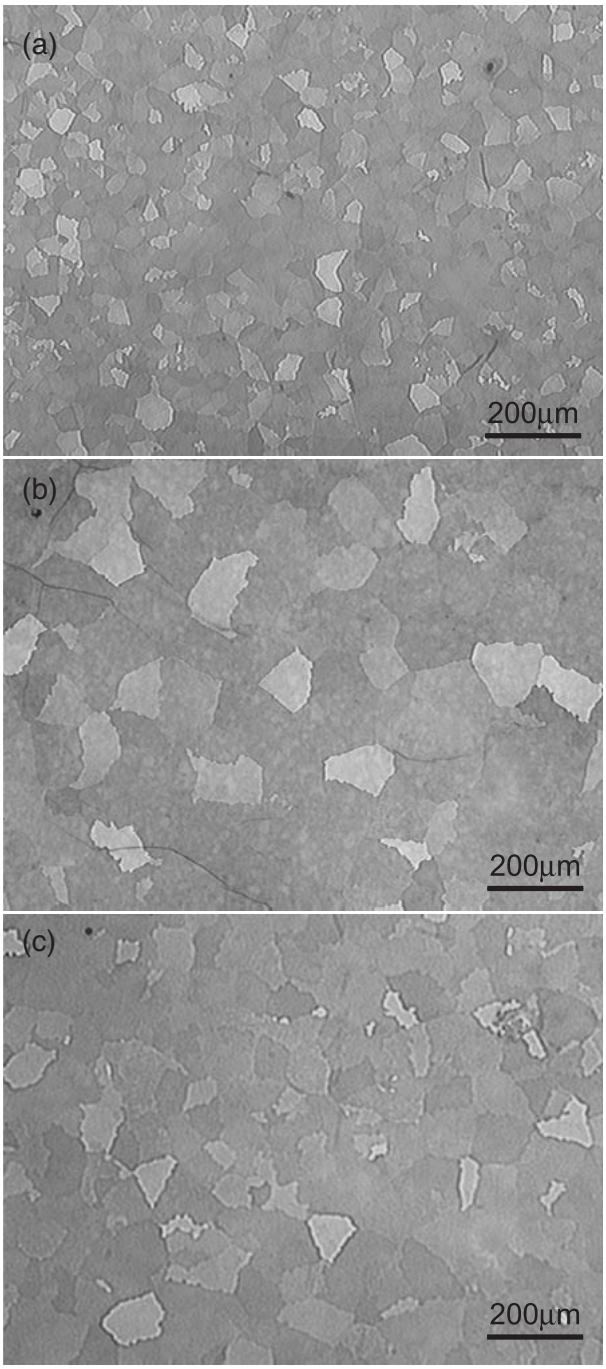

Fig. 8 Fully transformed microstructure for isothermal annealing at 973 K. (a) $Fe_{20.9}Si_{70.5}$, (b) $Fe_{27.14}Mn_{2.36}Si_{70.5}$, (c) $Fe_{28.91}Co_{0.59}Si_{70.5}$.

tion period and a prolonged induction time for the onset of the reaction, especially with the addition of Mn.

REFERENCES

1) I. Nishida: Phys. Rev. B **7** (1973) 2710–2713.
2) T. Kojima: Phys. Status Solidi A **111** (1989) 233–242.
3) U. Birkholtz and J. Schelm: Phys. Status Solidi **27** (1968) 413–425.
4) J. Hesse and R. Bucksch: J. Mater. Sci. **5** (1970) 272–273.
5) I. Yamauchi, H. Okamato, A. Suganuma and I. Ohnaka: J. Mater. Sci. **33** (1998) 385–394.
6) I. Yamauchi, T. Nagase and I. Ohnaka: J. Alloys Comp. **292** (1999) 181–190.
7) T. B. Massalsky (Ed.): *Binary Alloy Phase Diagram*, (ASM, Metals Park, Ohio, 1986) p. 1108.
8) T. Nagase, I. Yamauchi and I. Ohnaka: J. Alloys Comp. **316** (2001) 212–219.
9) T. J. Zhu, X. B. Zhao and S. H. Hu: J. Mater. Sci. Lett. **20** (2001) 1831–1833.
10) J. X. Jiang, K. Matsugi, G. Sasaki and O. Yanagisawa: Mater. Trans., JIM **46** (2005) 720–725.
11) J. Christian: *Theory of Transformation in metals and alloys*, (Pergamon Press, Oxford, 1975) pp. 433–489.
12) Z. Fan: Acta Metall. Mater. **43** (1995) 43–49.
13) J. Van Den Boomgaard: J. Iron Steel Inst. **210** (1972) 276–279.
14) J. Šestak: *Thermophysical Properties of Solids: Their Measurements and Theoretical Thermal Analysis*, (Elsevier, Amsterdam, 1984) p. 191.
15) M. Buchwitz, R. Adlwarth-Dieball and P. L. Ryder: Acta Metall. Mater. **41** (1993) 1885–1892.
16) B. O. Hildmann, H. Schneider and M. Schmücker: J. Eur. Ceram. Soc. **16** (1996) 287–292.